Adv. Polar Upper Atmos. Res., **20**, 63–75, 2006

Review

Ground-based radar detection of the equatorward boundary of ion auroral oval in the dusk-midnight sector and its dynamical association with substorms

P.T. Jayachandran[1]*, J.W. MacDougall[2] and E.F. Donovan[3]

[1]*Physics Department, University of New Brunswick, Fredericton, NB, Canada E3B 5A3*
[2]*Department of Physics and Astronomy, University of Western Ontario, London, ON, Canada*
[3]*Department of Physics and Astronomy, University of Calgary, Calgary, AB, Canada*
**Corresponding author. E-mail: jaya@unb.ca*

(Received January 26, 2006; Accepted May 8, 2006)

Abstract: One of the important boundaries of the auroral region in the dusk-midnight sector is the equatorward boundary of the ion precipitation. In this region, on average, the ion precipitation region is equatorward of the electron precipitation region and is important in the overall energy budget. There are ground and satellite based measurement techniques to detect this important boundary but many of these measurements lack the temporal and spatial coverage required to study the dynamical features of this boundaries relationship with substorms. In this paper a review of a new ground based radar technique to determine the boundary and its limitations are presented. The new radar method is used to study the substorm growth phase dynamics. It found that on average, the boundary is located more equatorward during substorms than during non substorms. This implies that magnetotail stretching is a necessary condition for substorms. It is also found that statically there is no difference in the location of the boundary for substorms and non substorms in the 18–19 hours magnetic local time sector. The equatorward expansion rate of the boundary shows clear distinction between substorms and non substorms: The equatorward expansion rate of the boundary is much lower during non substorms than during substorms. Implications of the results for substorm dynamics are also presented.

key words: auroral ionosphere, auroral substorms, particle precipitation, SuperDARN radar

1. Introduction

The terrestrial magnetosphere is a reservoir of different charged particle populations of varying energy. The magnetic field-aligned guiding center motion of these charged particles is in general quasi-periodic between two mirror points. Numerous processes act on these particles that can lower the altitude of these mirror pints allowing the particles to interact collisionally with atmospheric neutrals and ions. These collisions leave the atmospheric atoms, molecules and ions in excited states (in the case of electron aurora). In the case of proton precipitation, the collisions often involve charge

exchange, leaving the newly formed hydrogen atom in an excited state. Relaxation involves the emission of one or more characteristic photons, and the sum of these emissions comprise the aurora.

We do not completely understand the scattering and acceleration mechanisms that lower the mirror heights of the particles causing them to "precipitate". Particle precipitation is an important source of energy which affects the electrodynamical properties, dynamics, thermal structures, as well as the constituent distribution in the high latitude ionosphere and thermosphere. The regions of intense auroral activity produced by these particle precipitations are called the "auroral oval". As stated above, the auroral oval represents the footprint of precipitating ions as well as electrons. Over the years most scientific effort went into the studies related to the electron part of the precipitating particles since in most regions it carries most of the energy. However, there are occasions when the proton (ion) precipitation carries significant part of the energy input into the Earth's upper atmosphere (Galand *et al*., 2001). The cause of proton precipitation varies with magnetospheric regions and topology of the magnetic field lines (see Donovan *et al*., 2003 and references therein). Proton precipitation is significant throughout the auroral oval and is often the dominant particle energy source in the cusp and at the equatorward boundary of duskside auroral oval (Hardy *et al*., 1989; Galand *et al*., 2001; Newell *et al*., 2005). Usually the dusk-midnight sector ion precipitation region maps to the inner ion plasma sheet and on average its earthward limit maps to the equatorward boundary of the ion auroral oval (Newell *et al*., 1998, 2005; Jayachandran *et al*., 2002a, b, 2005). The most equatorward boundary of the auroral oval in the dusk-midnight sector is the location where high energy ions stops precipitating (*i.e.* the transition between bounce trapping and strong pitch angle scattering). The equatorward cutoff of ion precipitation corresponds to both the ion isotropy and b2i boundaries (Sergeev *et al*., 1993; Newell *et al*., 1996, 1998) and this boundary also corresponds to the equatorward boundary of proton aurora (Donovan *et al*., 2003). This boundary represents an important transition in the magnetosphere and its location depends on the topology of the inner magnetosphere (Donovan *et al*., 2003; Jayachandran *et al*., 2005). Since protons retain the large scale structure more efficiently than electrons, proton auroral measurements are an excellent probe for investigating magnetospheric substorms and Magnetosphere-Ionospheric (M-I) coupling process. Understanding the spatial and temporal dynamics of the dusk-midnight sector ion auroral boundary is crucial in understanding the dynamics of the inner magnetosphere relative to processes like substorms (Jayachandran *et al*., 2005) since most of the substorms occur in the duskmidnight sector of the auroral oval (Liou *et al*., 2001).

The most commonly used and reliable mean to measure the ion precipitation is the satellite based particle sensors used in the DMSP class of satellites (Hardy *et al*., 1989). The main disadvantage with the DMSP class satellite measurements, for the studies related to temporal and spatial dynamics of proton precipitation, is that the boundary is identified once during an oval crossing by the satellite, and hence no information about temporal evolution of the boundary is available on time scales less than typical times between crossings. Furthermore, the boundary is identified only on the satellite track, and so no information about the spatial structure of the boundary is obtained in this way.

The proton precipitation can be inferentially observed *via* the proton aurora that it causes. The SI-12 channel of the FUV instrument on IMAGE provides two minute cadence global images of the proton aurora *via* the Doppler shifted Lyman α (Mende *et al*., 2000). There are also two wavelengths produced by proton precipitation in the visible region (Balmer H_α and H_β). Monitoring H_α is problematic in that the line is very close to N_2 IP bands, which are bright in the electron auroral region (Chamberlain, 1961) and thus this technique demands very high spectral resolution. Ground-based instruments typically use the H_β line at 486.1 nm. Historically this line was detected by Vegrad (1939) and used extensively by Eather (1967, 1988) and recently by Donovan *et al.* (2003) to study the dynamics of the proton auroral boundary. This technique also has limitation in addressing the question related to the spatial dynamics of the proton aurora and its equatorward boundary since there are only limited number of ground based photometer appropriately located at different local time sectors of the auroral oval and any ground based optical measurements in the visible region demands clear sky conditions which limits the observations.

Auroral signatures can be observed in most of the electromagnetic spectrum including the radiowaves. The association between the optical auroral forms and coherent radiowave backscatter in varying frequency ranges is well established (Herlofson, 1947; Bates *et al*., 1969; Romick *et al*., 1974; Moeller, 1974; Hall *et al*., 1990; Milan *et al*., 2000) and these studies showed good temporal correlation between active optical auroral forms (associated with electron precipitation) and radiowave backscatter. Association between ion precipitation/proton aurora and coherent radiowave backscatter is not established until recently by Jayachandran *et al.* (2000). Jayachandran *et al.* (2000) have discovered that in the dusk-midnight sector of the auroral oval there exists a type of *E* region HF backscatter associated with ion precipitation. Jayachandran *et al.* (2000) used SuperDARN radar backscatter to show the association between *E* region backscatter in the dusk-midnight sector of the auroral oval and ion precipitation. SuperDARN (Greenwald *et al*., 1995) is an array of HF radars, which has wide area coverage and covers most of the northern and southern high-latitude regions. In this paper we will outline the SuperDARN based technique to determine the equatorward boundary of ion precipitation/proton aurora in the dusk-midnight sector of the auroral oval and its dynamical association with substorms.

2. SuperDARN radar technique to determine the equatorward boundary of ion precipitation and its validation with different measurements.

SuperDARN radars (Greenwald *et al*., 1995) are deployed to study the large scale ionospheric convection pattern in the high latitudes. These radars presently cover much of the high-latitude regions of the northern and southern hemisphere. These pulsed radars operate in the frequency range of 8–20 MHz. The radar antenna system consists of a main array of 16 log periodic antennas and an additional array of 4 antennas (the interferometer array, which is used for elevation angle measurements). The antennas of each array are electronically phased with one another to form an antenna pattern in which the maximum gain (beam position) has one of 16 azimuthal pointing directions separated by ~3.2°, distributed symmetrically about the radar bore-

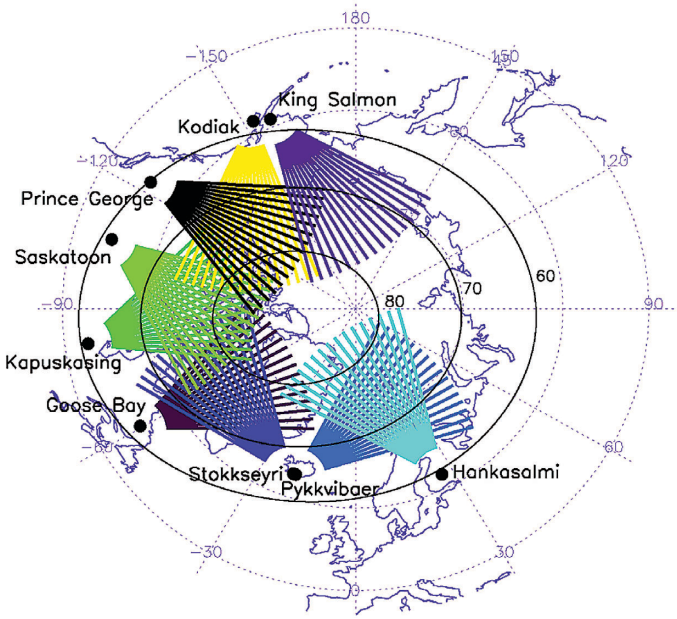

Fig. 1. Location of the Northern Hemisphere SuperDARN radars.

site. This configuration will yield 16 beam directions for each of the radars and with 9 radars in the Northern Hemisphere provides wide area coverage. SuperDARN was conceived of as a tool for monitoring convection on global scales. Figure 1 shows the location and area of coverage in the northern hemispheric radars, some of which are used for this study.

SuperDARN works on the principle of coherent backscatter from ionospheric plasma irregularities generated by different irregularity mechanisms. Since SuperDARN radars operate in the HF frequency range the condition for backscatter (radar wave must be perpendicular to magnetic field) can be met at *E* and *F* regions of the ionosphere because of refraction and the elevation angle measured by the interferometer array will be crucial in determining the location of the radar backscatter echoes. Figure 2 shows the statistics of SuperDARN radar echoes detected by the Saskatoon SuperDARN radar during three months (spring) of 1997 along with the elevation angle measurements. Figure 2a shows the magnetic local time—magnetic latitude occurrence distribution of all the ionospheric echoes and Fig. 2b shows corresponding elevation angle measurements. The echoes of interest to us the high-occurrence of near range echoes between 1800–2400 hrs local time. A close examination of the elevation angle reveals that these echoes are coming from low elevation angles and they are therefore *E* region echoes. A comparison of this figure with the ion precipitation statistics of ion precipitation using DMSP satellite particle measurements (Galand *et al*., 2001) reveals that the high concentration of these *E* region echoes corresponds to the region of high energy ion precipitation. Once the association between *E* region backscatter and ion precipitation is established the next logical step is to use this type of backscatter to determine the boundary

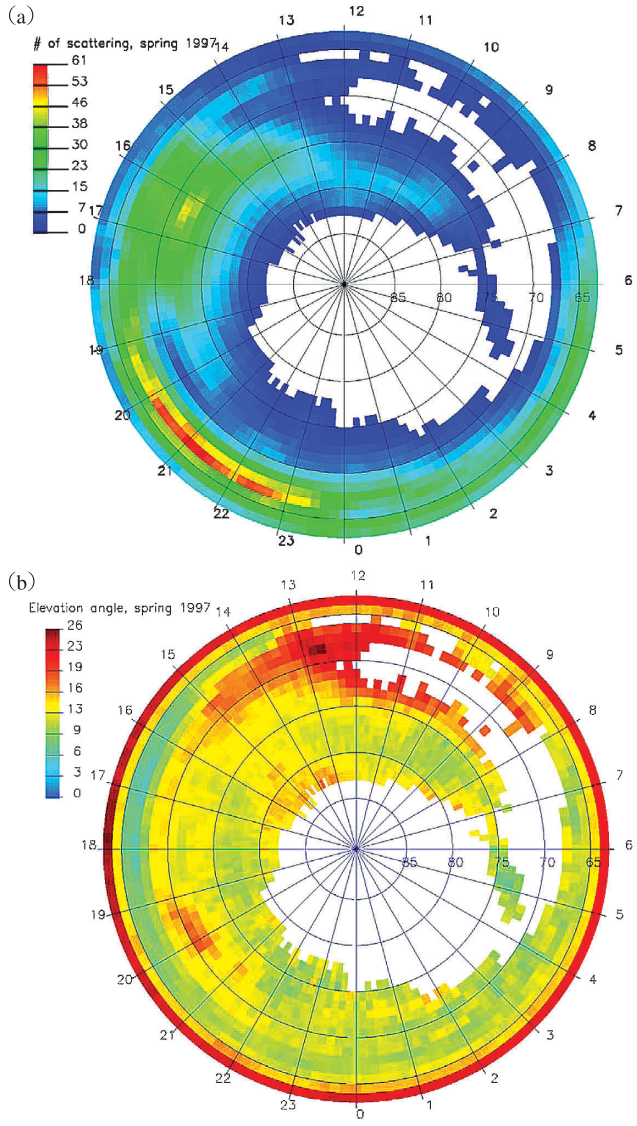

Fig. 2. Magnetic latitude—magnetic local time distribution of the occurrence of (a) backscatter and (b) corresponding elevation angle for SuperDARN Saskatoon radar during the spring months of 1997.

of *E* region backscatter and see whether this boundary corresponds to any important particle boundaries.

Jayachandran *et al.* (2002a) compared the location of the equatorward boundary of SuperDARN *E* region backscatter with DMSP particle boundaries and concluded that the equatorward boundary of these *E* region backscatter corresponds to the b2i boundary (equatorward boundary of high energy ion precipitation). A later study by

Sotirelis *et al.* (2005) reached the same conclusion that equatorward boundary of radar backscatter corresponds to the equatorward boundary of ion precipitation in the dusk midnight sector. Jayachandran *et al.* (2002b) also compared the location of the radar backscatter boundary with the equatorward boundary determined using ground H_β measurements and concluded that the two boundaries corresponds well and shows that temporal behavior of these two boundaries follow each other very well. Figure 3 shows the distribution of the boundaries determined by the (a) radar, (b) DMSP satellite, and (c) ground based Meridian Scanning photometer respectively. The mean and standard deviation for each distribution is given in each figures. Even though these are not simultaneous observation the distribution shows similar patterns and confirms earlier results of Jayachandran *et al.* (2002a, b) and Sotirelis *et al.* (2005) that in the dusk-midnight sector SuperDARN radar backscatter boundary can be used as a proxy for the b2i boundary. One factor to keep in mind is that the radar data used for this study has latitudinal limitations (lower limit of Mag. Lat. 62.5°N due to the location of the radar and higher limit of 68.5°N due to the maximum latitude of obtaining direct *E* region backscatter).

Association between *E* region backscatter and ion precipitation in the duskmidnight sector can be linked with the plasma instability mechanism and the geometrical conditions for the radiowave backscatter. Since we are dealing with SuperDARN, which operates at HF, vertical gradients of the ionization play an even more important role in the generation of irregularities than at VHF (St.-Maurice *et al.*, 1994). The associa-

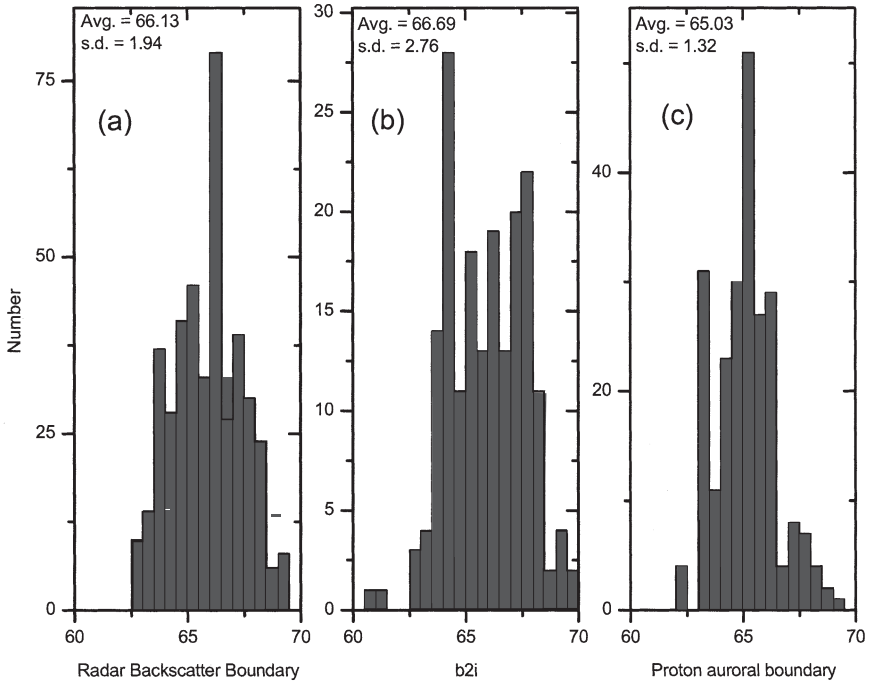

Fig. 3. Distribution of the boundaries determined by (a) radar (b) DMSP satellite, and (c) H_β emission.

tion of observed *E* region irregularities with proton aurora and high-energy ion precipitation suggests that these irregularities are formed through the gradient drift mechanism. The H_β emissions are due primarily to several to tens of keV precipitating CPS protons, which deposit most of their energy in the *E* region (Vontrat-Reberac *et al*., 2001), and produce steep gradients in electron density. This gradient, and a properly directed electric field make the *E* region unstable through the gradient drift instability mechanism and produces irregularities and thus radiowave backscatter. Generally, in the dusk–midnight sector of the auroral oval, the electric field is directed northward and the bottom side of the *E* region is unstable through the gradient drift instability mechanism. Further, the absence of *E* region backscatter if the H_β intensity is <20R and the disappearance of the backscatter if the electric field changes its directions also confirm that the generation mechanism of these irregularities is the gradient drift instability.

It should be emphasized that other factors such as refraction and radar geometry (location) affects the detection of HF irregularities. This can have important consequence in the detection of *E* region backscatter and identification of the boundary. So far we have analyzed the SuperDARN data from the Saskatoon, Kapuskasing and Goose Bay SuperDARN radars to identify the equatorward boundary of the auroral oval using the *E* region backscatter. Uspensky *et al.* (2001) has also reported the presence of "ribbon echoes" (narrow region of *E* region backscatter) from the diffuse auroral region using the SuperDARN Finland radar. For the Finland radar, the geometry is different from other radars, the incident radar wave is almost perpendicular to the magnetic field (condition required for radio backscatter) without refraction, implying that refraction actually produces a negative effect (bends the ray away from perpendicularity). Hence the irregularities are detected only from the region where there is no refraction (region where the ray is orthogonal to the isoelectron density surface). This is in contrast to the Saskatoon, Kapuskasing, and Goose Bay radars for which the incident rays are a few degrees from the normal and refraction is necessary to obtain perpendicularity. A detailed study is required to determine which of the other SuperDARN radars (in northern and southern polar regions) can actually determine the auroral boundary taking all the factors into consideration.

3. Boundary dynamics associated with substorms

The boundary undergoes diurnal, seasonal and transient variations associated with substorms (Newell *et al*., 1998). Figure 4 show some examples of latitude-time variations of backscatter velocity detected using the Saskatoon SuperDARN radar. Location of the most equatorward backscatter is the location of the boundary. Three examples clearly show variability in the boundary dynamics. For example from Fig. 4b it can be seen that the boundary does not show much equatorward expansion at all; whereas Fig. 4c shows a rapid expansion and Fig. 5b shows relatively slow expansion. It clearly shows that boundary undergoes different dynamical behavior. The diurnal and seasonal variations are predictable and will not be discussed in this paper.

It is well known that during substorm growth phase the auroral oval expands equatorward and so does the boundary. This equatorward motion of the boundary during the substorm growth phase is attributed to thinning and earthward motion of the

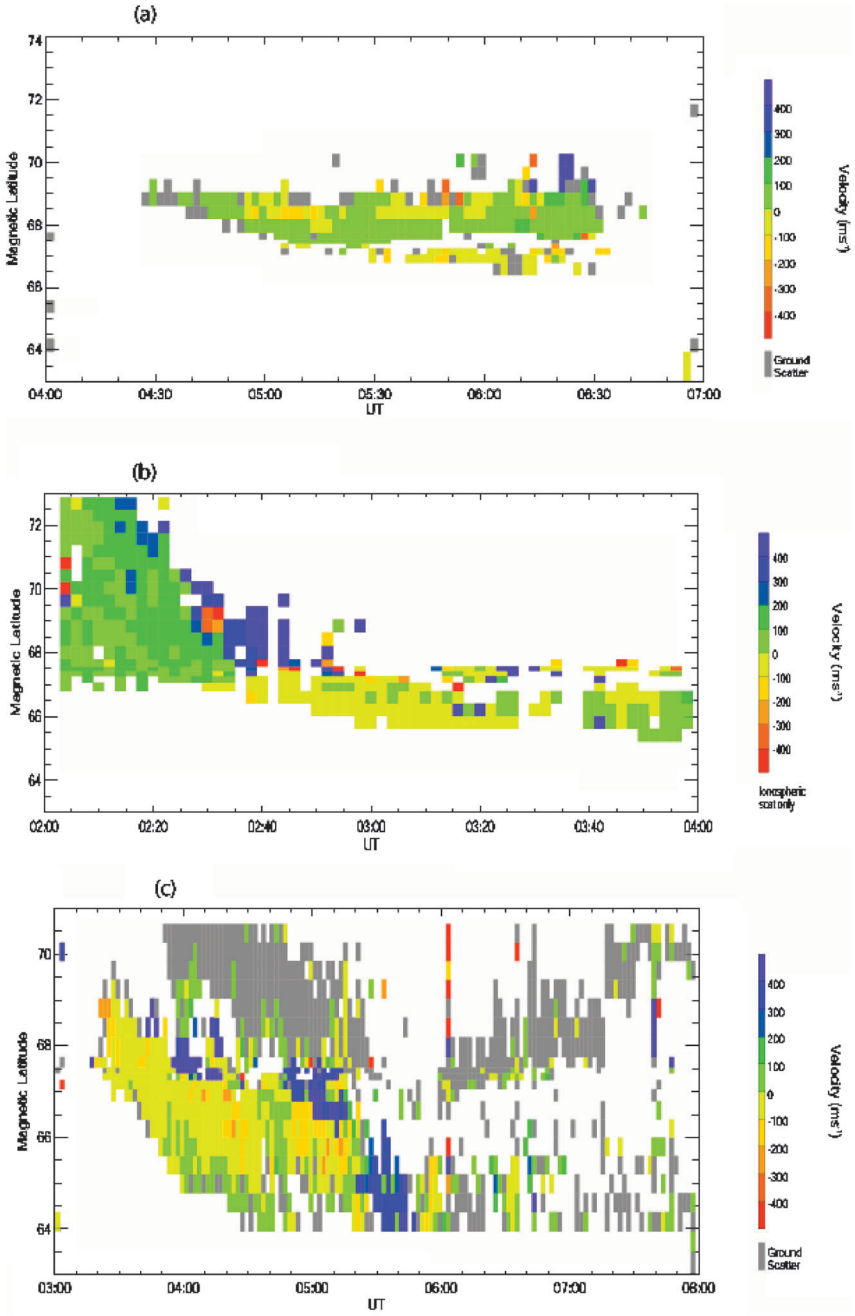

Fig. 4. Three typical examples showing the latitude–velocity–time plot of SuperDARN backscatter Doppler velocity. Location of the most equatorward edge of the backscatter is the location of the boundary discussed in this paper.

cross-tail current in the inner magnetosphere as the field evolves towards a more stretched topology (Sergeev *et al*., 1993; Roux *et al*., 1991). A high degree of correlation between the location of the boundary and the magnetic field inclination at geo-synchronous orbit (Newell *et al*., 1998; Donovan *et al*., 2003) proves that the location indicates the stretching of the magnetotail. A recent study by Jayachandran *et al.* (2005), using the advantage of the spatial coverage of the SuperDARN, have shown that there are at least two qualitatively different and distinct types of expansion of the boundary during substorm growth phase. The first is "global equatorward expansion" of the boundary, in which the boundary expanded equatorward self-similarly in all local time sectors in the dusk-midnight sector. The second is "local equatorward expansion", in which there is an azimuthally limited region where the boundary moves equatorward, likely indicated an azimuthally limited Earthward intrusion of the inner edge of the plasma sheet.

These studies points to the fact that a close examination of the boundary dynamics during substorm growth phase may give some clues regarding the substorm dynamics and their generation mechanisms. In this paper we are going to address the boundary dynamics purely with respect to substorm perspective and not taking in to account of other external drivers such as the solar wind and Interplanetary Magnetic Field (IMF). For this purpose we have used the same data sets used by Jayachandran *et al.* (2002c, 2005). Substorms onsets and their location are identified using the Polar UVI data as discussed by Liou *et al.* (2001). We have considered only the substorms whose onset occurred between 21–23 local time regions, is in the vicinity of the Kapuskasing radar field of view, and between 62°–70°N magnetic latitudes (in the Canadian sector). Location of the boundary is identified using the Goose Bay, Kapuskasing, and Saskatoon radars. We have also used H_β data from Gillam (Mag. Lat. 67.47°N) and Pinnawa (Mag. Lat. 61.15°N) to determine the boundary location using the technique used by Donovan *et al.* (2003). We have considered isolated substorms only, which we identify as times when there was no brightening during $\pm$3 hours around the onset in question. We have also used magnetometer and photometer data to confirm the onset of the substorm and not for any other purpose such as determining the onset time and onset location. We have binned the boundary location determined from the radars and photometers in half hour bins and separated the time history of boundary location for substorm cases and non substorm cases. We have classified the case as a non substorm case only when there is POLAR data and we did not observe onset brightening.

Figure 5 shows the statistical plot of the location of the boundary (a) determined from the radars and (b) determined using the photometers. Combination of three radars gives measurement of the boundary in nine local time sectors whereas the photometer gives measurement of the boundary in one local time. Radar data shows the snapshot of the boundary location 15 min prior to the onset of the substorm. Since the photometer provides data for a single meridian there is a convolution of spatial and temporal behaviors of the boundary. The idea behind this figure is to show the similarities in the boundary behavior determined by the radar and the photometer. Main data for this paper is the radar data. Error bars in the figure represents the standard deviation. Standard deviation in the photometer data is high because of fewer data points and gives an one point measurement in local time as far as the location of the boundary is concerned. The plots show a clear difference in the location of the boundary for substorm

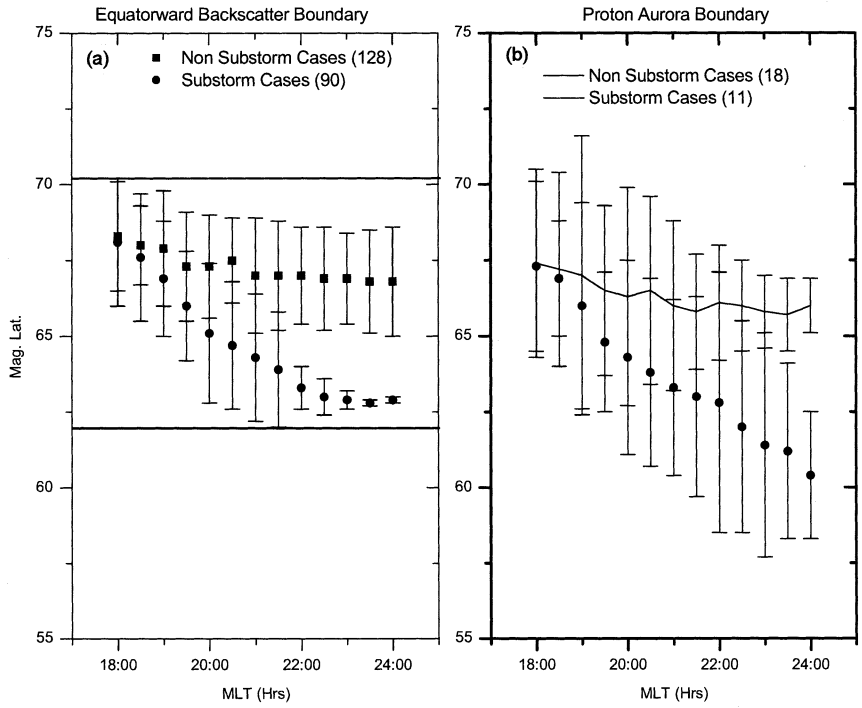

Fig. 5. Statistics of the time history of the location of the boundary for substorm cases and non substorm cases (a) using radar and (b) using H_β emission. Error bars are the standard deviations. Horizontal lines in the graph showing the radar boundary represents the lower and upper limits of the boundary location that can be detected by the radar.

and non substorm cases are concerned. The boundary was located at lower latitudes for substorm cases and at higher latitudes for no substorm cases (the location of the boundary for substorm cases after 2230 hours local time is an artifact of the location of the radars). This clearly points to the fact that magnetic field stretching is an essential condition for most of the substorm cases. Another interesting feature to point out here is that in the local time sector between 18–19 hours there is not much difference in the location of the boundary for substorms and non substorm cases, which may indicate that the field lines threading this region have the same topology for substorms and no substorms.

The combination of three radars will allow us to determine the equatorward expansion rate of the boundary for substorm and non substorm cases, which may give us some clues related to the dynamics. Figure 6 shows the distribution of the average equatorward expansion rate of the boundary calculated 15 min prior to the onset. The average expansion rate is estimated for the 30 min interval 15 min prior to the identified onset. This condition (15 min prior) is applied to avoid the late growth phase local expansion of the boundary prior to a type of substorms as discussed by Jayachandran *et al.* (2005). For no substorm cases the average expansion rate between 2200 and 2300 magnetic local times is calculated and used as average expansion rate. Figure 6 shows

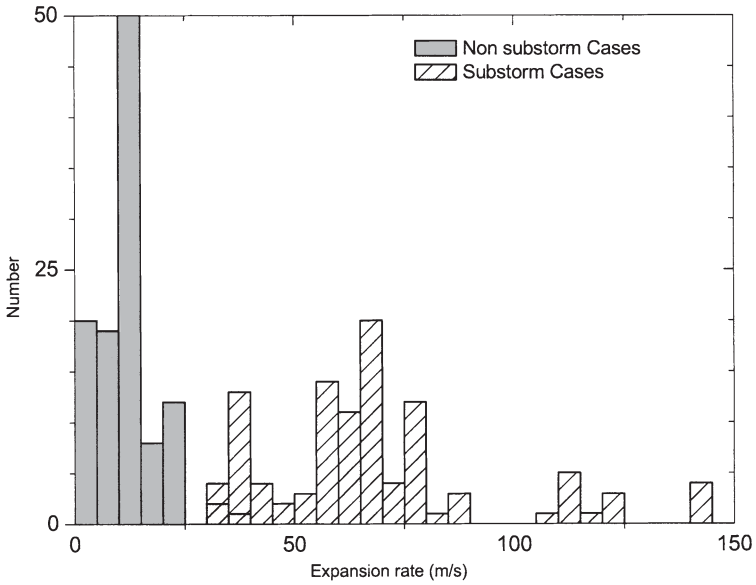

Fig. 6. Equatorward expansion rate of the boundary for substorm and non substorm cases.

the expansion rate of the boundary for substorms and non substorm cases. A remarkable feature which is obvious from the figure is the separation of the expansion rate for substorm and non substorm cases. No substorm expansion rates are grouped at lower speeds ($<$35 m/s) and substorm expansion rates are higher and are highly variable (there is a very small overlap region). This clearly indicates that even though dynamics of the boundary associated with substorms are highly variable there is clear distinction between expansion rate for substorm and non substorm cases.

The equatorward motion of this boundary during the substorm growth phase is attributed to thinning and earthward motion of the cross-tail current in the inner magnetosphere as the field evolves towards a more stretched topology (Sergeev *et al*., 1993; Roux *et al*., 1991). Newell *et al.* (1998) and Donovan *et al.* (2003) have shown a high-degree of correlation between the magnetic field inclination at geo-synchronous orbit and the location of the boundary. Growth phase stretching is generally agreed to be a consequence of the loading of magnetic flux into the tail, which in turn is a consequence of energy entering the magnetospheric system through dayside merging at a rate greater than it can be transported through the nightside magnetotail *via* the standard convection cycle (see *e.g*., Baker *et al*., 1999, and references therein). The observed difference in the expansion rate could be possibly related to the factors such as the rate of energy input into the tail, rate of change of convection in the tail, or the difference between the antisunward convection and return convection (difference in the energy input and the energy transport within the tail). Although complete understanding of what this difference in the rate of the equatorward expansion signifies will require more thorough study, these empirical results indicate that the prediction of substorm onset location may be possible by the combination of the location of the boundary location and the equator-

ward expansion rate of the boundary.

4. Conclusion

Equatorward boundary of *E* region backscatter of some of the SuperDARN radars can be used to detect the equatorward boundary of high-energy ion precipitation in the dusk-midnight sector of the auroral oval. This boundary coincides with the ion isotropy boundary and b2i boundary determined using different techniques. The new radar technique has an advantage of wide area coverage and is a useful tool in the investigation of the spatial and temporal dynamics of the boundary associated with substorms. A study of the boundary dynamics as related to substorms reveal that on average the boundary is located at lower latitude for substorms and at higher latitudes for non substorms clearly indicating that magnetotail stretching is an essential condition for most of the substorm onsets. There is clear distinction between the expansion rate of the boundary for substorm and non substorms. The expansion rate of the boundary is lower for non substorms and higher for substorms. A thorough study is required to understand the factors that control the equatorward expansion rate of the boundary.

Acknowledgments

This research was supported by grant from Natural Science and Engineering Research Council (NSERC) of Canada. We acknowledge the Canadian Space Agency and Fokke Creutzberg for the CANOPUS MSP data.

The editor thanks Dr. K. Hosokawa and another referee for their help in evaluating this paper.

References

Baker, D.N., Pulkkinen, T.I., Buchner, J. and Klimas, A.J. (1999): Substorms: A global instability of the magnetosphere-ionosphere system. J. Geophys. Res., **104**, 14601–14611.

Bates, H.F., Sharp, R.D., Belon, A.E. and Boyd, J.S. (1969): Spatial relationship between HF radar aurora, optical aurora and electron precipitation. Planet. Space. Sci., **17**, 83–95.

Chamberlain, J.W. (1961): Physics of the Aurora and Airglow. New York, Academic Press, 704 p.

Donovan, E.F., Jackel, B.J., Voronkov, I., Sotirelis, T., Creutzberg, F. and Nicholson, N.A. (2003): Ground-based optical determination of the b2i boundary: A basis for an optical MT-index. J. Geophys. Res., **108**, 1115, doi: 10/1029/2001JA009198.

Eather, R.H. (1967): Auroral proton precipitation and hydrogen emissions. Rev. Geophys., **5**, 207–285.

Eather, R.H. (1988): Results from Antarctic optical studies. Rev. Geophys., **26**, 579–590.

Galand, M., Fuller-Rowell, T.J. and Codescu, M.V. (2001): Response of the upper atmosphere to auroral proton. J. Geophys. Res., **106**, 127–139.

Greenwald, R.A. *et al.* (1995): DARN/SuperDARN: A global view of the dynamics of high-latitude convection. Space. Sci. Rev., **71**, 761–796.

Hall, G.E., Moorcroft, D.R., Cogger, L.L. and Andre, D. (1990): Spatial relationship between large aspect angle VHF radio aurora and 557.7 nm emissions: Evidence for refraction. J. Geophys. Res., **95**, 15281–15288.

Hardy, D.A., Gussenhoven, M.S. and Brautigam, D. (1989): A statistical model of auroral ion precipitation. J. Geophys. Res., **94**, 370–392.

Herlofson, N. (1947): Interpretation of radio echoes from polar auroras. Nature, **160**, 867–868.

Jayachandran, P.T., St.-Maurice, J.-P., MacDougall, J.W. and Moorcroft, D.R. (2000): HF detection of slow long-lived *E* region plasma structures. J. Geophys. Res., **105**, 2425–2442.

Jayachandran, P.T., MacDougall, J.W., St.-Maurice, J.-P., Moorcroft, D.R., Newell, P.T. and Prikryl, P. (2002a): Coincidence of the ion precipitation boundary with the HF *E* region backscatter boundary in the dusk-midnight sector. Geophys. Res. Lett., **29** (8), 10.1029/2001GL014184.

Jayachandran, P.T., Donovan, E.F., MacDougall, J.W., Moorcroft, D.R., St.-Maurice, J.-P. and Prikryl, P. (2002b): SuperDARN *E* region backscatter boundary in the dusk-midnight sector—Tracer of the equatorward boundary of the auroral oval. Ann. Geophys., **20**, 1899–1904.

Jayachandran, P.T., MacDougall, J.W., Moorcroft, D.R., St.-Maurice, J.-P., Liou, K. and Newell, P.T. (2002 c): Substorm onset locations and the equatorward boundary of the proton auroral oval. Geophys. Res., Lett., **29** (24), 2159, doi.1029/2002GL015484.

Jayachandran, P.T., Donovan, E.F., MacDougall, J.W., Moorcroft, D.R., Liou, K., Newell, P.T. and St.-Maurice, J.-P. (2005): Global and local equatorward expansion of the ion auroral oval before substorm onsets. J. Geophys. Res., **110**, A05204, doi: 10.1029/2004JA010837.

Liou, K., Newell, P.T., Sibeck, D.G. and Meng, C.-I. (2001): Observation of IMF and seasonal effects in the location of auroral substorm onset. J. Geophys. Res., **106**, 5799–5810.

Mende, S.B., Heetderks, H., Fry, H.U. *et al.* (2000): Far ultraviolet imaging from the IMAGE spacecraft: 3. Spectral imaging of Lyman-α and OI 135.6 nm. Space Sci. Rev., **91**, 287–318.

Milan, S.E., Lester, M., Sato, N., Takizawa, H. and Villain, J.-P. (2000): Investigation of the relationship between optical auroral forms and HF radar *E* region backscatter. Ann. Geophys., **18**, 608–617.

Moeller, H.G. (1974): Backscatter results from Lindau, II, The movements of curtains of intense irregularities in the polar *F* layer. J. Atmos. Terr. Phys., **36**, 1487–1501.

Newell, P.T., Feldstein, Y.I., Galperin, Y.I. and Meng, C.-I. (1996): Morphology of nightiside precipitation. J. Geophys. Res., **101**, 10737–10748.

Newell, P.T., Sergeev, V.A., Bikkuzina, G.R. and Wing, S. (1998): Characterizing the state of the magnetosphere: Testing the ion isotropy boundary maxima latitude (b2i) and the ion isotropy boundary. J. Geophys. Res., **103**, 4739–4745.

Newell, P.T., Wing, S., Sotirelis, T. and Meng, C.-I. (2005): Ion aurora and its seasonal variations. J. Geophys. Res., **110**, A01215, doi: 10.1029/2004JA010743.

Romick, G.J., Ecklund, W.L., Greenwald, R.A., Balsley, B.B. and Imhof, W.L. (1974): Interrelationship between the $>$130 keV electron trapping boundary, the VHF radar backscatter, and the visual aurora. J. Geophys. Res., **79**, 2439–2443.

Roux, A.S., Perraut, S., Robert, P., Morane, A., Pedersen, A., Korth, A., Kremser, G., Aparicio, B., Rodgers, D. and Pellinen, R. (1991): Plasma sheet instability related to the westward traveling surge. J. Geophys. Res., **96**, 17697–17714.

Sergeev, V.A., Mitchell, D.G., Russell, C.T. and Williams, D.J. (1993): Structure of the tail plasma/current sheet at ~11 R_E and its changes in the course of a substorm. J. Geophys. Res., **98**, 17345–17366.

Sotirelis, T., Ruohoniemi, J.M., Barnes, R.J., Newell, R.T., Greenwald, R.A., Skura, J.P. and Meng, C.-I. (2005): Comparison of SuperDARN radar boundaries with DMSP particle precipitation boundaries. J. Geophys. Res., **110**, A06302, doi: 10.1029/2004JA010732.

St.-Maurice, J.-P., Prikryl, P., Danskin, D.W., Hamza, A.M., Sofko, G.J., Koehler, J.A., Kustov, A.V. and Chen, J. (1994): On the origin of narrow non-ion-acoustic coherent radar spectra in the high-latitude *E* region. J. Geophys. Res., **99**, 6447–6474.

Uspensky, M., Eglitis, P., Opgenoorth, H., Starkov, G., Pulkkinen, T. and Pellinen, R. (2001): On auroral dynamics observed by HF radar: 1. Equatorward edge of the afternoon-evening diffuse luminosity belt. Ann. Geophys., **18**, 1560–1575.

Vegard, L. (1939): Hydrogen showers in the auroral region. Nature, **144**, 1089–1090.

Vontrat-Reberac, R., Fontaine, D.R., Blelly, P.L. and Galand, M. (2001): Theoretical predictions of the effect of cusp and dayside precipitation on the polar ionosphere. J. Geophys. Res., **106**, 28857–28865.